INSTITUTE OF PHYSICS PUBLISHING NANOTECHNOLOGY
Nanotechnology **17** (2006) 5033–5037 doi:10.1088/0957-4484/17/20/001

Functionalization of individual ultra-short single-walled carbon nanotubes

Jared M Ashcroft, Keith B Hartman, Yuri Mackeyev, Cristina Hofmann, Sean Pheasant, Lawrence B Alemany and Lon J Wilson

Department of Chemistry, R E Smalley Institute for Nanoscale Science and Technology, and the Center for Biological and Environmental Nanotechnology MS 60, Rice University, Houston, TX 77251-1892, USA

E-mail: durango@rice.edu

Received 25 June 2006, in final form 8 August 2006
Published 22 September 2006
Online at stacks.iop.org/Nano/17/5033

Abstract

We report the functionalization of individual ultra-short (20–80 nm lengths) single-walled carbon nanotubes (US-tubes) via *in situ* Bingel cyclopropanation. Upon chemical reduction (K°/THF) of bundled US-tubes, the bundling forces are electrostatically overcome to yield single, negatively charged US-tubes in solution. These single US-tubes can then be functionalized with malonic acid bis-(3-*tert*-butoxycarbonylaminopropyl) ester using Bingel chemistry (CBr_4/DBU) to yield 4–5 adducts nm^{-1}, as determined by x-ray photoelectron spectroscopy (XPS). The derivatized US-tubes remain as individuals after functionalization and charge quenching. Thermogravimetric analysis (TGA) and solid-state NMR spectroscopy confirmed covalent attachment of the adducts and indicated tight wrapping of the adduct arms about the US-tubes. The resulting debundled and derivatized US-tubes serve as a prototype single-molecule-like 'capsule' for the containment and delivery of medically-useful payloads.

(Some figures in this article are in colour only in the electronic version)

M Supplementary data files are available from stacks.iop.org/Nano/17/5033

1. Introduction

Single-walled carbon nanotubes (SWNTs) show promise for many applications due to their unique chemical and physical properties [1]. One area of emerging interest is biomedical applications [2]. However, the length, bundling and functionalization of SWNTs must first be controlled for SWNTs to realize their full potential in medicine, as well as other fields.

The majority of nanotube research has focused on full-length SWNTs. However, it has been demonstrated recently that SWNTs can be shortened via fluorination and subsequent pyrolysis in argon to yield cut, ultra-short carbon nanotubes (US-tubes), with most lengths ranging between 20 and 80 nm [3]. These US-tube lengths may be especially useful for medical applications as recent work has suggested an inverse relationship between nanorod length and mammalian cellular uptake [4], and it is well established that particle size plays an important role in renal elimination with smaller particles being eliminated more readily than larger particles of the same material [5, 6]. In fact, a US-tube-based contrast agent (Gd_n^{3+}@US-tubes) for magnetic resonance imaging (MRI) has been shown to outperform classical clinical agents by up to two orders of magnitude [7]. In addition, US-tubes have been shown to possess twice the surface area of full-length SWNTs and to retain radiolabelled I_2 for 1–2 orders of magnitude longer than full-length SWNTs [8]. Thus, there is growing interest in US-tube materials. Although US-tubes can be produced by other methods [9], we are especially interested in those obtained by the F_2/pyrolysis procedure because the procedure creates sidewall defects through which various agents may be internally loaded [7, 8].

A major hurdle that plagues both full-length SWNTs [10] and US-tubes [3b] is the tendency to bundle, which impedes solubility, and thus the development of individualized SWNT platforms for various applications. The π–π stacking

 © 2006 IOP Publishing Ltd Printed in the UK

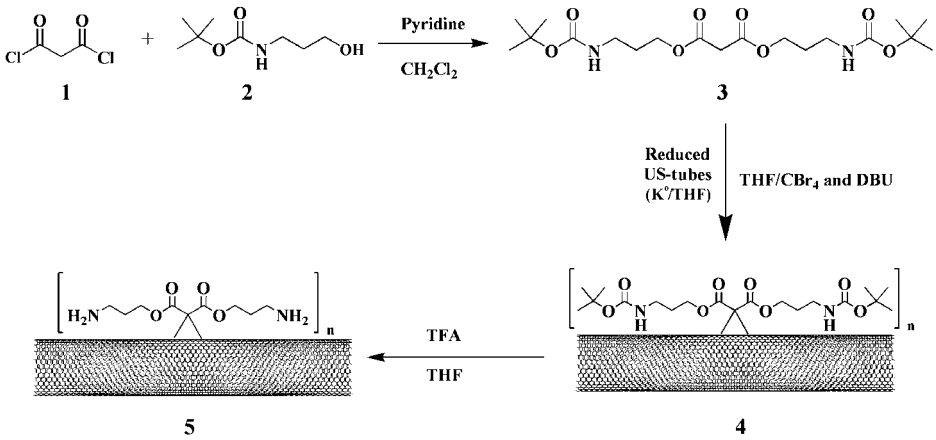

Figure 1. Sidewall derivatization of individual (reduced) US-tubes by Bingel chemistry; $n = 4$–5 nm^{-1}.

interactions between different SWNTs results in aggregated bundles which have a van der Waals binding energy of ∼0.5 eV nm^{-1} of tube–tube contact [11]. Debundling and subsequent water suspension of SWNTs has been achieved with sonication and by wrapping them in polymers, such as polyvinyl pyrrolidone (PVP) and polystyrene sulfonate (PSS) [12], and surfactants, like sodium dodecyl sulfate (SDS) [13]. Unfortunately, these methods do not work well for suspending US-tubes.

The current model of SWNT dispersion in solution postulates that sonication separates full-length SWNTs at the tube ends because they possess large length:width aspect ratios, imparting relative flexibility. Once a surfactant or polymer wraps around a tube end, it can propagate along the bundle length, eventually separating bundled nanotubes into individual, surfactant-coated nanotubes [14]. US-tubes, on the other hand, are so short (<80 nm) that they act more as rigid rods making the usual method of debundling futile because there is insufficient torque to peel the tubes from one another. Therefore, alternative methods are needed to individualize US-tubes.

Full-length SWNTs can be exfoliated by fluorination with F_2(g) to form fluoronanotubes [15] or by chemical reduction to form salts of highly charged (8–10 e^-/nm) SWNTs [16]. We have adapted the latter procedure in this work to exfoliate US-tubes into single, highly charged US-tubes in K°/THF and then derivatize the resulting singles with *in situ* Bingel chemistry so as to sterically prevent rebundling. The Bingel reaction is a widely used method for derivatizing fullerenes of the C_{60} class, which involves cyclopropane ring formation across a [6, 6′] fullerene bond using a bromomalonate and NaH [17a]. A modified version of the reaction, called Bingel–Hirsch, employs CBr_4 and DBU as a base, eliminating the need for isolation and purification of a bromomalonate [17b]. The Bingel reaction has also been used to functionalize the sidewalls of bundled full-length SWNTs [18]. However, the reaction has not been used to derivatize US-tubes and, in fact, no sidewall derivatization of any nature has been reported to date for a US-tube prepared by the F_2/pyrolysis procedure. This paper describes one such method whereby functionalized, individual US-tubes are prepared by chemical reduction (K°/THF), followed by immediate derivatization by Bingel chemistry in a single *in situ* procedure [17a].

2. Experimental details

Raw HiPco SWNTs [19] were fluorinated in a Monel flow apparatus using a gaseous mixture of 1% F_2 in He at 50 °C for 2 h, a condition which yields F-SWNTs with a stoichiometry of CF_x ($x \leqslant 0.2$) [3a]. Under an argon atmosphere, the F-SWNTs were then pyrolysed in a tube furnace at 1000 °C for 2 h to drive off volatile fluorocarbons, yielding chemically cut US-tubes. Upon cooling, the sample was bath sonicated in concentrated HCl for 30 min to remove the iron catalyst impurities. This process produced bundled US-tubes with average lengths of ∼40 nm, with ∼80% of them shorter than 60 nm [3b] and with a residual iron content of less than 1.5% by mass, as determined by thermogravimetric analysis (TGA).

An amended Birch reduction was used to chemically reduce the US-tubes by first adding 30 mg of US-tubes to 150 ml of dry THF in an argon-purged 250 ml round bottom flask. Chemical reduction was accomplished by the addition of 200 mg of potassium, followed by 2 h of sonication. The resulting, reduced US-tubes were soluble in THF for up to 10 days with no visible precipitation. The US-tube/THF solution was then decanted from the reaction flask to remove unreacted potassium and to prepare the US-tubes for the Bingel reaction.

Bingel functionalization of the reduced US-tubes was carried out by addition of 2.0 g of **3** (figure 1), prepared by a literature procedure [20], to the reduced US-tube/THF solution. The reaction then proceeded by the addition of 2.5 g of CBr_4 and 1.5 g of DBU to the solution with subsequent sonication for one hour, followed by stirring overnight. The solvent was then removed under reduced pressure and the solid washed with THF and diethyl ether until the decant was clear. After washing, the solid was placed in a 35 °C oven and dried overnight to yield 10 mg of **4** (figure 1). The yield was 33% based on US-tubes. Deprotection of the protected amine groups of **4** was accomplished by adding 5 ml of TFA to 10 mg of the compound in 5 ml of THF. The reaction was sonicated for 1 h and subsequently washed three times

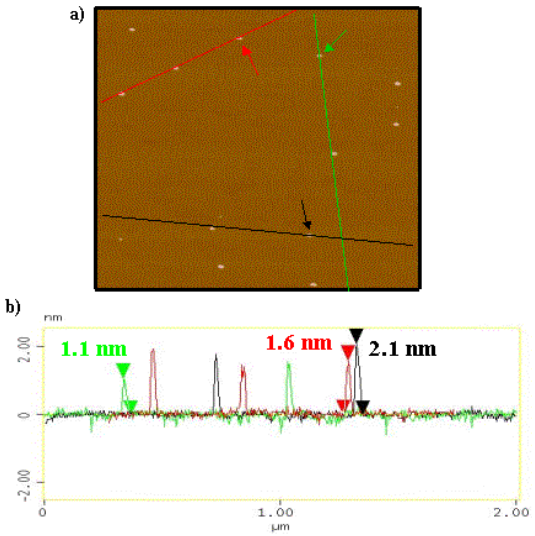

Figure 2. (a) AFM height image of **4** and (b) z-scan resolution height analysis of **4**.

with THF and diethyl ether to yield 10 mg of **5** (figure 1). The same reaction sequence was also performed on non-reduced US-tubes in order to compare characterization of the two functionalized US-tube materials. The water solubility of **5** was determined by UV–vis spectroscopy at pH 7. First, the material was dissolved in 500 μl of water to give a 0.400 mg ml^{-1} solution. This solution was then diluted to achieve a range of concentrations and a spectrum was recorded for each. The point at which the spectra ceased to be linear ($R^2 = 0.995$) in intensity with increasing concentration was deemed to be the water solubility of **5**.

ATR-IR spectroscopy, TGA, XPS, Raman spectroscopy, AFM and NMR spectroscopy were used to characterize the US-tube derivatives and to determine the extent of derivatization. ATR-IR spectra were obtained on a Nicolet Avatar 370 FT-IR spectrometer with an ATR attachment by pressing a US-tube sample (KBr pellet) onto a Ge crystal. TGA analysis was performed by placing a 2–3 mg US-tube sample into a platinum crucible and ramping the temperature at 5 °C min^{-1} from room temperature to 700 °C under argon. Raman spectroscopy data were collected at 633 nm using a Renishaw Raman Microscope. XPS analysis was performed on a Phi Quantera XPS spectrometer; solid samples were prepared by pressing them onto indium foil. AFM analyses were performed using a DI Nanoscript 3A instrument in tapping mode for US-tube samples in order to compare degrees of debundling; the samples were spin coated on a mica wafer after dispersion and sonication in THF.

Solid-state ^{13}C NMR spectra were obtained on a Bruker AVANCE-200 NMR spectrometer (50.3 MHz ^{13}C, 200.1 MHz ^{1}H) described previously [21]. The basic ^{1}H–^{13}C CPMAS spectrum was obtained with 7 kHz MAS, a 1 ms contact time, 29.3 ms FID, and 5 s relaxation delay. The FID obtained after 48 400 scans was processed with 50 Hz (1 ppm) of line broadening. The dipolar dephasing spectrum differed from the basic ^{1}H–^{13}C CPMAS spectrum in that after CP, two 25 μs dephasing periods with a 180° ^{13}C refocusing pulse in the middle were used before FID acquisition in order to eliminate the methylene signals. The FID obtained after 67 600 scans was processed with 50 Hz of line broadening. Chemical shifts are reported relative to the carbonyl carbon of glycine defined as 176.46 ppm [22].

Table 1. XPS results for the US-tube materials. Numbers are in at.% with an instrument error of 0.5%.

Sample	C (%)	F (%)	N (%)	K (%)	O (%)
US-tubes (unreduced)	90.4	0.9	0.5	0.0	8.0
Bingelated US-tubes (unreduced)	91.8	0.3	2.0	0.0	5.9
US-tubes (reduced)	75.3	0.6	0.4	12.5	10.5
Bingelated US-tubes (reduced)	86.4	0.3	3.5	1.2	8.1

3. Results and discussion

The reaction sequence in figure 1 has been used to demonstrate the exfoliation and functionalization of individual US-tubes. The particular malonate in figure 1 was chosen because it is well characterized in the literature [20], it contains nitrogen for XPS studies (see below), its primary-amine form in **5** makes individual US-tubes water-soluble (see below), and it is a good choice for linking US-tubes to other materials of biological interest (e.g. peptides or antibodies) [23].

The extent of exfoliating by the K°/THF reduction and subsequent derivatization of US-tubes was assessed by AFM (figure 2 and supporting information available at stacks.iop.org/Nano/17/5033). Comparing z-resolution heights of US-tubes and their derivatives yields insight into the relative bundling of each species. A single HiPco full-length SWNT on average is 1.0 nm in diameter, though variances may be from 0.5 to 2.0 nm [24]. AFM analyses of freshly cut US-tubes measured z-resolution heights in excess of 7.0 nm, clearly demonstrating extensive bundling (figure S-1, supporting information available at stacks.iop.org/Nano/17/5033). In comparison, the K°/THF reduced US-tubes showed z-resolution heights ranging from 0.5–1.5 nm which corresponds to individualized US-tubes (figure S-2, supporting information available at stacks.iop.org/Nano/17/5033). AFM z-resolution height measurements of **4** ranged from 1.1 to 2.1 nm (figure 2), clearly demonstrating that the Bingel functionalized US-tubes do not re-bundle and exist as single-molecule-like species.

It would be expected that reduced US-tubes would functionalize to the maximum extent possible due to their greater exposed surface area. Raman spectroscopy analysis of compound **4** demonstrated an increase in intensity of the sp^3-hybridized carbon peak at ~1290 cm^{-1} for the derivatized US-tube sample, as compared to an underivatized sample (figure S-3, supporting information available at stacks.iop.org/Nano/17/5033). These Raman spectroscopy results serve to demonstrate the integrity of the US-tube material both before and after derivatization (both have a spectrum characteristic of an SWNT) and to indicate successful addition of the malonate groups to the US-tube sidewalls. XPS has been used to further determine the extent of Bingel functionalization by measuring the increased nitrogen content in the sample upon the formation of **4**. This increase was approximately 3% (table 1). For comparison, the Bingel reaction was also performed on unreduced, bundled US-tubes,

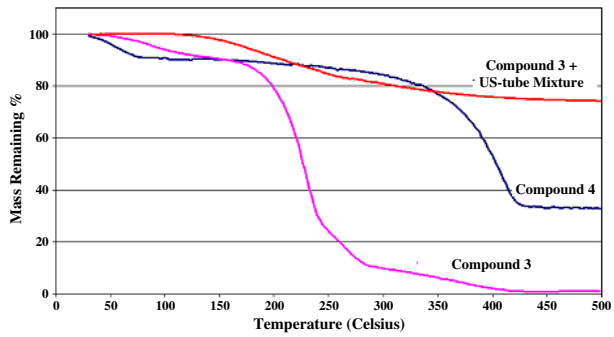

Figure 3. TGA data for compounds **3**, **4** and a mixture of **3** plus US-tubes.

which demonstrated only moderate functionalization with an increase in nitrogen atomic per cent of 1.5%. Thus, the reduced (single) US-tubes show greater functionalization relative to unreduced (bundled) US-tubes, as anticipated. A second and then third Bingel reaction performed on the same sample of compound **4** found that the nitrogen percentage plateaued at about 5%. Assuming that 1 nm of a US-tube contains 120 carbons, approximately 4–5 Bingel groups are added per nanometre of US-tube, which agrees well with observed mass increase after functionalization. The observed high oxygen content of the sample is likely due to the presence of oxygen (epoxides or carboxylates) on the ends or defect sites of the US-tubes (Raman spectroscopy shows considerable sp^3 character in the US-tube starting material, a consequence of the cutting procedure) and/or to residual solvent or adsorbed water.

Compound **4** was characterized by ATR-IR spectroscopy, TGA and NMR spectroscopy. The ATR-IR spectrum (figure S-4, supporting information available at stacks.iop.org/Nano/17/5033) showed a strong C=O stretch at 1736 cm^{-1}. This corresponds to carbonyl ester groups from the Bingel malonate attached to the US-tube. TGA analysis of compound **4** showed that as the temperature is increased to 350 °C, the malonate groups cleave from the US-tubes (figure 3). Data were also obtained for a US-tube/compound **3** mixture (no covalent attachment) for comparison purposes. This data showed that **3** volatilized by 200 °C, supporting the argument that the loss of mass for **4** is indeed from covalently attached malonates. After cleavage, approximately 40% of the sample mass remained, indicating that approximately 60% of the mass is due to the Bingel malonate groups. This is consistent with the data acquired from XPS, which also indicated attachment of approximately 4–5 Bingel groups nm^{-1} of US-tube. The initial loss of ∼8% mass of compounds **3** and **4** is likely due to unremoved solvent or water.

The basic ^1H–^{13}C CPMAS spectrum of compound **4** (figure 4) indicates sp^3 and sp^2 functionalities. The upfield portion of the aliphatic signal results from overlapping signals from the *t*-butyl methyl carbons and two of the three different types of methylene carbons. A peak maximum of 26 ppm is upfield of what would be expected for such carbons [20] and indicates that the US-tube is exerting a shielding effect on the addend [21]. The downfield tail of the aliphatic signal is consistent with overlapping signals from the different quaternary carbons of the cyclopropane ring, the methylene carbon adjacent to oxygen, and the *t*-butyl quaternary carbon

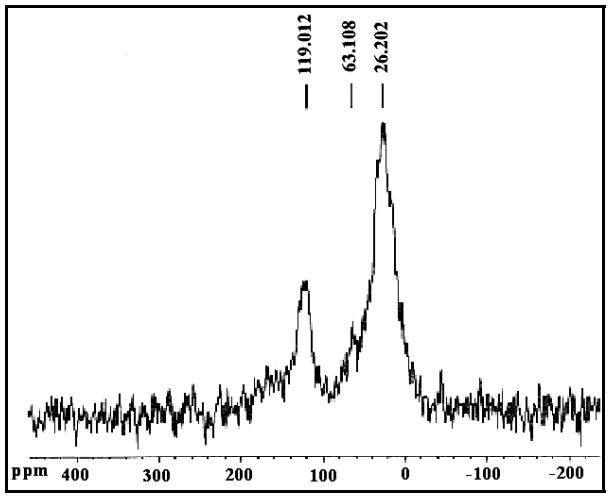

Figure 4. ^1H–^{13}C CP-MAS NMR spectrum of compound **4**.

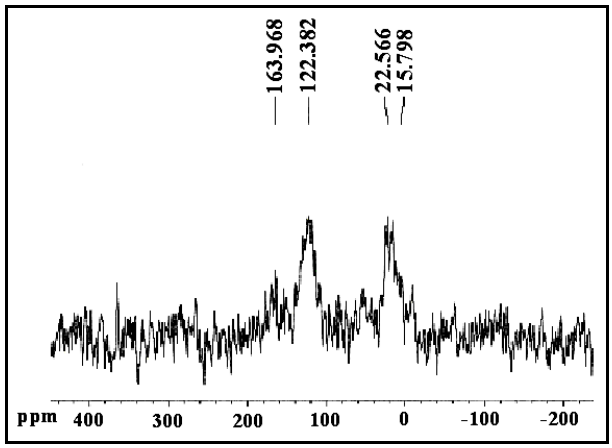

Figure 5. Dipolar dephasing NMR spectrum of compound **4**.

(also adjacent to oxygen). The carbons of the cyclopropane ring can be expected to give relatively weak signals in light of their distance from the nearest protons, while the *t*-butyl quaternary carbon can be expected to give a relatively weak signal resulting from weak ^1H–^{13}C dipole–dipole interactions with the highly mobile methyl protons [25]. The prominent sp^2 signal at about δ120 clearly results from unfunctionalized sp^2 carbons of the US-tube, while its downfield tail is consistent with overlapping signals from the carbamate and ester carbonyl carbons. The signal at about δ120 can reasonably arise from cross polarization from methylene protons of the addend lying along the US-tube, a particularly clear example of the through-space nature of cross polarization.

The CPMAS spectrum with a pair of 25 μs dephasing periods (figure 5) displays only attenuated signals from methyl and quaternary carbons. The *t*-butyl methyl signals are clearly weak after only 50 μs of dephasing [25]; this may reflect only partial cross polarization with just a 1 ms contact time before the dephasing process. Lengthening the contact time to 3 ms did not result in a detectable aliphatic signal after 17 400 scans, which suggests that $T_{1\rho}$ (H) is no more than a few milliseconds. Regardless, peak maxima at about 15–20 ppm (TMS as 0 ppm)

are clearly upfield of what would be expected for *t*-butyl methyl carbons, as these signals are at δ29 in the precursor malonate or correspondingly functionalized C_{60} [20]. The other types of quaternary aliphatic carbon would give signals further downfield. The US-tube is clearly exerting a shielding effect on the addend. The very shielded nature of the *t*-butyl methyl carbons is consistent with the malonate group being in close proximity to the nanotubes—perhaps tightly wrapped around the tube—although we cannot rule out the possibility of *t*-butyl methyl carbons on a given nanotubes being unusually shielded because of close proximity to other nanotubes. These NMR data strongly suggest that covalent functionalization of the Bingel US-tubes was achieved.

Finally, compound **4** was deprotected to obtain **5** as shown in figure 1. Following cleavage of the *t*-Boc protecting group, a positive Kaiser test verified that a primary amine was indeed present, as had been previously observed for amine-derivatized full-length SWNTs [26]. The water-solubility of **5** was determined by UV–vis spectroscopy to be approximately 0.25 mg ml^{-1}, as described in the experimental details section.

4. Conclusion

Unlike full-length SWNTs, ultra-short SWNTs (US-tubes) cannot be debundled into single entities in aqueous solution by the usual surfactant/sonication procedures. However, debundling and sidewall derivatization of US-tubes can be accomplished by *in situ* Bingel–Hirsch chemistry under strongly reducing conditions. We believe that this is an important step in the development of US-tube materials because single US-tubes can now be highly derivatized, and the subsequent material is a single-molecule-like 'capsule' which is capable of further manipulation (e.g. filling). Our interest lies in using these capsules as building blocks for the development of carbon nanoprobes for medical imaging and therapy. The recently reported high-performance Gd_n^{3+}@US-tube MRI contrast agent [7] is a prime example of the type of advanced medical materials that might be derived from US-tubes, and such materials are most attractive when individual, derivatized species are available.

Acknowledgments

This research was supported by the Robert A Welch Foundation (Grant C-0627), Carbon Nanotechnologies, Inc. (Houston, TX), the NASA Johnson Space Center and University of Texas Health Science Center (Grant NNJ05HE75A), and the Center for Biological and Environmental Nanotechnology (NSF EEC-0118007) at Rice University; KBH is a CBEN Graduate Student Fellow.

Supporting information available from
stacks.iop.org/Nano/17/5033

AFM analysis of US-tubes (figure S-1)

AFM analysis of reduced US-tubes (figure S-2)

Raman spectra of US-tubes and compound 4 (figure S-3)

FI-IR spectrum of compound 4 (figure S-4).

References

[1] Dresselhaus G and Avouris P (ed) 2001 *Carbon Nanotubes: Synthesis, Structure, Properties and Applications* (New York: Springer)
[2a] Martin C R and Kohli P 2003 *Nat. Rev. Drug Discovery* **2** 29
[2b] Lin Y, Taylor S, Li H, Fernando K A S, Qu L, Wang W, Gu L, Zhou B and Sun Y 2004 *J. Mater. Chem.* **14** 527
[3a] Mickelson E T, Huffman C B, Rinzler A G, Smalley R E, Hauge R H and Margrave J L 1998 *Chem. Phys. Lett.* **296** 188
[3b] Gu Z, Peng H, Hauge R H, Smalley R E and Margrave J L 2002 *Nano Lett.* **2** 1009
[3c] Khabashesku V N, Billups W E and Margrave J L 2002 *Acc. Chem. Res.* **35** 1087
[4] Chithrani B D, Ghazani A A and Chan W C W 2006 *Nano Lett.* **6** 662
[5] Chang R L S, Ueki I F, Troy J L, Deen W M, Robertson C R and Brenner B M 1975 *Biophys. J.* **15** 887
[6] Oliver J D, Anderson S, Troy J L, Brenner B M and Deen W M 1992 *J. Am. Soc. Nephrol.* **3** 214
[7] Sitharaman B *et al* 2005 *Chem. Commun.* **31** 3915
[8] Mackeyev Y A, Marks J W, Rosenblum M G and Wilson L J 2005 *J. Phys. Chem.* B **109** 5482
[9] Kam N W, Jessop T C, Wender P A and Dai H 2004 *J. Am. Chem. Soc.* **126** 6850
[10] Thess A *et al* 1996 *Science* **273** 483
[11] Girifalco L A, Hodak M and Lee R S 2000 *Phys. Rev.* B **62** 13104
[12] O'Connell M J, Boul P, Ericson L M, Huffman C, Wang Y, Haroz E, Kuper C, Tour J, Ausman K D and Smalley R E 2001 *Chem. Phys. Lett.* **342** 265
[13a] O'Connell M J *et al* 2002 *Science* **297** 593
[13b] Moore V C, Strano M S, Haroz E H, Hauge R H and Smalley R E 2003 *Nano Lett.* **3** 1379
[14] Strano M S, Moore V C, Miller M K, Allen M J, Haroz E H, Kittrell C, Hauge R H and Smalley R E 2003 *J. Nanosci. Nanotechol.* **3** 81
[15] Mickelson E T, Chiang I W, Zimmerman J L, Boul P J, Lozano J, Liu J, Smalley R E, Hauge R H and Margrave J L 1999 *J. Phys. Chem.* B **103** 4318
[16a] Liang F, Sadana A K, Peera A, Chattopadhyay J, Gu Z, Hauge R H and Billups W E 2004 *Nano Lett.* **4** 1257
[16b] Pénicaud A, Poulin P, Derré A, Anglaret E and Petit P 2005 *J. Am. Chem. Soc.* **127** 8
[17a] Bingel C 1993 *Chem. Ber.* **126** 1957
[17b] Camps X and Hirsch A 1997 *J. Chem. Soc., Perkin Trans.* **1** 1595
[18a] Coleman K S, Bailey S R, Fogden S and Green M L H 2003 *J. Am. Chem. Soc.* **125** 8722
[18b] Worsley K A, Moonoosawmy K R and Kruse P 2004 *Nano Lett.* **4** 1541
[19] Nikolaev P, Bronikowski M J, Bradley R K, Rohmund F, Colbert D T, Smith K A and Smalley R E 1999 *Chem. Phys. Lett.* **313** 91
[20] Richardson C F, Schuster D I and Wilson S R 2000 *Org. Lett.* **2** 1011
[21] Peng H, Alemany L B, Margrave J L and Khabashesku V N 2003 *J. Am. Chem. Soc.* **125** 15174
[22] Hayashi S and Hayamizu K 1991 *Bull. Chem. Soc. Japan* **64** 685
[23] Ashcroft J M, Tsyboulski D A, Hartman K B, Zakharian T Y, Marks J W, Weisman R B, Rosenblum M G and Wilson L J 2006 *Chem. Commun.* 3004 (doi:10.1039/b601717g)
[24] Kim U J, Gutièrrez H R, Kim J P and Eklund P C 2005 *J. Phys. Chem.* B **109** 23358
[25] Alemany L B, Grant D M, Pugmire R J, Alger T D and Zilm K W 1983 *J. Am. Chem. Soc.* **105** 2142
[26] Georgakilas V, Tagmatarchis N, Pantarotto D, Bianco A, Briand J-P and Prato M 2002 *Chem. Commun.* **28** 3050